



# University Library

Author/Filing Title ..... SHIGIDI, I.M.T.A

Class Mark ..... T

**Please note that fines are charged on ALL  
overdue items.**

FOR REFERENCE ONLY

0403603358





# **A Study of the Bubble Point Test for Membrane Characterisation**

**Ihab M. T. A. Shigidi**

**A Doctoral Thesis submitted in partial fulfilment of  
the requirements for the award of Doctor of  
Philosophy degree of Loughborough University.**

Advanced Separation Technologies Group,  
Department of Chemical Engineering,  
Loughborough University,  
Loughborough, Leicestershire,

UK.

May 2007.

© Ihab Shigidi.



Loughborough  
University  
Pilkington Library

Date

8/2008

Class

T

Acc

No. 0403603358

## **Acknowledgement**

I wish to express my deepest gratitude to my supervisors Professor Richard Wakeman and Professor Vahid Nassehi for their invaluable advice, supervision and support throughout this research.

I am also grateful to the Department of Chemical Engineering, Loughborough University for providing the financial support for this work. Special thanks to Mr Chris Manning for his technical help during the experimental work.

I would also like to thank my friends and colleagues in David Collett hall specially Mr Jonathan Hansford, Paul Cantwell, Sheryl Williams, June Beswick, Jackie Grant, Dace Rozenberga and specially Dr Parviz Behrouzi for offering me the subwarden position in David Collett Hall.

I am also thankful to my friends Dr M.G. Hassan, Dr K. Al-Hakim, and Dr Nazar Abdalkareem for their constructive suggestions and assistance during my residency in Loughborough. The unceasing support and encouragement of my parents and brothers have been a constant motivation for me to strive ahead in my research towards the completion of my Ph.D. research.

## *Abstract*

---

---

Filtration is a commonly used separation process. Many researchers have looked at the different properties affecting the performance of filter media and many methods have been considered for testing their efficiency. The performance of a filtration process is mainly dependent on the status of the filter medium and its ability to act as perfect barrier within the process, and from there arose the importance of defining its properties and integrity.

In this research we are looking at the bubble point test as one of the more useful, economical tests for examining a particular type filter medium. 0.2  $\mu\text{m}$ , 5  $\mu\text{m}$  and 12  $\mu\text{m}$  Nuclepore track etched membranes were used in this research as their pore dimensions are close to cylindrical. The main parameters investigated were the minimum and mean pore size in addition to the bubble point. Two types of porometers were used in this research, the PMI and the Coulter II, and the results obtained by both were in good agreement with the ranges specified by the manufacturers.

The selection of Nuclepore track etched membranes is made due to the uniqueness of the shapes of their pores. The cylindrical shape of the pores in this type of membranes simplifies the approach towards modelling the bubble point test, and thus understanding the microhydrodynamics occurring inside the membrane. This knowledge is obtained from this research by simulating both velocity and pressure profiles as well as gas-liquid interaction inside single and multiple pores, thus providing comprehensive understanding on the behaviour of the gas and the liquid

phase inside the membrane. Such knowledge will help improve the design for a better system to accurately measure the bubble point test.

Different mathematical methods can be applied, but the ability of the penalty scheme finite element method in dealing with complex geometries and such complex phenomena made it the preferred method. On the other hand the use of the volume of fluid method to detect the interfacial surface between the gas and the wetting liquid inside a pore microstructure has not been fully addressed before and thus considered as a novel part of this research.

## *Table of Contents*

---

---

Certifficat of origniality	
Acknowledgement	
Abstract	
Table of Contents.....	1
List of Figures.....	6
Nomenclature.....	10
Nomenclature.....	10
Chapter 1 Introduction.....	12
1.1. Preliminary Remarks.....	12
1.2. Research Objectives and Practical Significance.....	14
1.3. Thesis Structure.....	15
Chapter 2 Literature Review.....	17
2.1. Microfiltration.....	17
2.2. Membrane types.....	17
2.2.1. Depth membrane filter.....	17
2.2.1.1. Depth membrane production.....	18
2.2.2. Track-etched membranes.....	19
2.2.2.1. Track etched membrane production.....	21
2.3. Pores.....	21
2.4. The characterisation of porous membranes.....	23
2.4.1. Mercury porosimetry.....	24
2.4.2. Thermoporometry.....	25
2.4.3. Permporometry.....	25



2.4.4. NMR measurements.....	27
2.4.5. Light transmission method.....	27
2.4.6. Scanning electron microscopy (SEM) .....	28
2.4.7. Atomic force microscopy (AFM) .....	28
2.4.8. Permeability method .....	29
2.4.9. Gas adsorption-desorption .....	29
2.4.10. Bubble pressure breakthrough .....	30
2.4.11. Glass bead challenge test .....	31
2.5. Measuring the pore size distribution.....	33
2.5.1. Porometer theory.....	33
2.6. Membrane integrity.....	34
2.6.1. Methods of measuring membrane integrity .....	36
2.6.1.1. Direct integrity tests.....	37
2.6.1.1.1. Air pressure decay testing (PDT).....	37
2.6.1.1.2. Diffusive air flow test .....	39
2.6.1.1.3. Bubble point test .....	40
2.6.1.2. Indirect integrity monitoring tests.....	40
2.6.1.2.1. Turbidity monitoring or reduction monitoring .....	40
2.6.1.2.2. Laser turbidity test .....	40
2.6.1.2.3. Particle counters.....	40
2.6.1.2.4. Conductivity tests.....	41
2.7. Gas Capillary Flow .....	43
2.7.1. Hagen-Poiseuille Model.....	44
2.7.2. Knudsen Model.....	44
2.7.3. Knudsen- Poiseuille Model.....	44

Chapter 3 Experimental Evaluation .....	48
3.1. Interaction of porous material with liquid .....	48
3.2. Wetting liquid displacement .....	49
3.3. Measurement technique .....	51
3.4. Automated Porometers.....	52
3.4.1. PMI Capillary Flow Porometer.....	54
3.4.2. Coulter II Porometer .....	57
3.5. Porometry Concerns.....	60
Chapter 4 Mathematical Modelling .....	63
4.1. Mathematical Model .....	63
4.2. Mathematical Modelling Strategies .....	64
4.3. The Finite Element Method .....	66
4.4. The volume of fluid method (VOF).....	70
4.5. Assumptions.....	71
4.6. Governing equations .....	73
4.7. Penalty Scheme .....	75
4.8. Calculation of Pressure .....	78
4.9. Boundary Conditions .....	79
4.9.1. Inlet boundary conditions .....	79
4.9.2. Outlet boundary conditions.....	79
4.9.3. Wall slip boundary conditions .....	80
4.10. Solution of Transient Equations.....	82
4.11. Developed Algorithm.....	84
Chapter 5 Experimental Results and Discussions.....	86
5.1. Coulter II Experimental Results.....	86

5.2. PMI Capillary Flow Porometer.....	96
5.3. Comparison between PMI and Coulter II porometers .....	100
Chapter 6 Numerical Results and Discussions .....	107
6.1. Input file format .....	108
6.2. Presentation of Results.....	108
6.3. Physical Data .....	108
6.4. Hydrodynamics inside a single pore .....	109
6.4.1. Velocity profile for single pore.....	110
6.4.2. Pressure profile for single pore .....	110
6.4.3. Gas flow inside a single pore .....	111
6.5. Dimensions and boundary conditions for multiple pores domain B.....	113
6.5.1. The effect of Penalty parameter .....	114
6.5.2. Velocity profile for multiple pores domain B.....	116
6.5.3. Pressure profile for multiple pores domain B .....	117
6.5.4. Gas flow inside multiple pores domain B.....	117
6.6. Dimensions and boundary conditions for multiple pores domain C.....	120
6.6.1. Hydrodynamics inside multiple pores domain C.....	121
6.6.2. Gas flow inside multiple pores domain C.....	122
6.7. Dimensions and boundary conditions for domain D .....	124
6.8. Dimensions and results for domain E .....	127
6.8.1. Hydrodynamics inside domain E.....	127
6.9. Dimensions and results for domain F .....	129
6.9.1. Slip boundary conditions results for domain F .....	129
6.9.2. No slip boundary condition results for domain F .....	131
6.10. Comparisons between experimental and numerical data.....	134

Chapter 7 Conclusions and recommendations for future work .....	140
7.1. Conclusion .....	140
7.2. Recommendations.....	143
References.....	145
Appendix 1.....	158
Appendix 2.....	159
Appendix 3.....	160
Appendix 4.....	245
Appendix 5.....	246
Appendix 6.....	247
Appendix 7.....	251
Appendix 8.....	253
Appendix 9.....	255

## *List of Figures*

---

---

Figure (2-1) Depth membrane filters. ....	18
Figure (2-2) Depth membrane production .....	19
Figure (2-3) Track etched membrane .....	20
Figure (2-4) Track etched membrane production .....	21
Figure (2-5) Types of pores .....	22
Figure (3-1) Empty and wetted through pores.....	48
Figure (3-2) Displacement of wetting liquid in the pores.....	49
Figure (3-3) Contact angel.....	51
Figure (3-4) Flow Porometry.....	56
Figure (3-5) Description of the Coulter II Porometer.....	60
Figure (4-1) Slip at a solid wall. ....	81
Figure (5-1) SEM image for 12 $\mu\text{m}$ Nuclepore track etched membrane sample.....	87
Figure (5-2) Wet, dry and half dry flow for 0.8 $\mu\text{m}$ sample using Coulter II porometer. .....	88
Figure (5-3) Diameter vs. Pressure for 12 $\mu\text{m}$ sample.....	90
Figure (5-4) Differential flow obtained at various pore diameters for 12 $\mu\text{m}$ sample.	90
Figure (5-5) Cumulative pore flow for 12 $\mu\text{m}$ sample.....	91
Figure (5-6) Differential pore diameter for 12 $\mu\text{m}$ sample. ....	92
Figure (5-7) Reproducibility of the Coulter II. ....	94
Figure (5-8) Cumulative flow for 5 $\mu\text{m}$ samples. ....	95
Figure (5-9) Differential flow for 5 $\mu\text{m}$ samples.....	95
Figure (5-10) Wet, dry and half dry flow for 5 $\mu\text{m}$ sample using PMI porometer. ....	96
Figure (5-11) Diameter vs. pressure for a 0.2 $\mu\text{m}$ sample. ....	97

Figure (5-12) Pore size distribution for 0.2 $\mu\text{m}$ sample. ....	98
Figure (5-13) Pore size distribution and cumulative flow for 0.2 $\mu\text{m}$ sample. ....	98
Figure (5-14) Maximum, minimum and mean pore size diameters for different 0.2 $\mu\text{m}$ samples.....	99
Figure (5-15) Mean flow pore diameter for 5 $\mu\text{m}$ samples using PMI and Coulter II porometers.....	100
Figure (5-16) Mean pore Size for 12 $\mu\text{m}$ samples using PMI and Coulter II porometers.....	101
Figure (5-17) Maximum pore Size for 12 $\mu\text{m}$ samples using PMI and Coulter II porometers.....	102
Figure (5-18) Maximum pore Size for 5 $\mu\text{m}$ samples using PMI and Coulter II porometers.....	103
Figure (5-19) Minimum pore size for 5 $\mu\text{m}$ samples using PMI and Coulter II porometers.....	104
Figure (5-20) Minimum pore size for 12 $\mu\text{m}$ samples using PMI and Coulter II porometers.....	104
Figure (5-21) Pore size distribution for 0.2 $\mu\text{m}$ sample tested 3 times.....	105
Figure (5-22) Cumulative flow for 0.2 $\mu\text{m}$ sample tested 3 times.....	105
Figure (6-1) Coloured magnitude scale .....	108
Figure (6-3) Velocity profile inside a single 1 $\mu\text{m}$ pore diameter .....	110
Figure (6-4) Simulated flow field and pressure distribution within a single 1 $\mu\text{m}$ pore with an inlet pressure of 11 kPa.....	111
Figure (6-5) The air-liquid interface at different times for a 1 $\mu\text{m}$ diameter pore and a non-slip boundary condition. ....	112
Figure (6-6) Dimensions for domain B.....	113

Figure (6-7) Velocity profile for domain B with penalty parameter $6 \times 10^{10}$ . .....	114
Figure (6-8) Velocity profile for domain B with penalty parameter $7 \times 10^{14}$ . .....	115
Figure (6-9) Velocity profile for domain B with penalty parameter $7.5 \times 10^{13}$ . .....	116
Figure (6-10) Pressure profile for multiple pores domain B.....	117
Figure (6-11A) Gas-liquid boundary inside multiple pore domain B.....	118
Figure (6-11B) Gas-liquid boundary inside multiple pore domain B.....	119
Figure (6-11C) Gas-liquid boundary inside multiple pore domain B.....	120
Figure (6-12) dimensions for domain C.....	121
Figure (6-13) Pressure profile for multiple pores domain C.....	121
Figure (6-14) Velocity profile for multiple pores domain C. ....	122
Figure (6-15) Gas liquid interfacial boundary inside equal pores at different time steps.....	123
Figure (6-16) Dimensions of multiple pore domain D. ....	124
Figure (6-17) Velocity profile for multiple pore domain D.....	125
Figure (6-18) Interfacial gas liquid boundary inside domain D at 4 different time steps.....	126
Figure (6-19) Dimensions of domain E. ....	127
Figure (6-20) Velocity and pressure profile inside multiple pore domain E. ....	128
Figure (6-21) Dimensions for multi-pores domain F.....	129
Figure (6-22) gas liquid displacement inside domain F using slip boundary conditions. ....	131
Figure (6-23) Simulated vector flow field in multi-pores domain F .....	131
Figure (6-24) Simulated pressure profile in multi-pores domain F with inlet of 0.1 kPa.....	132

Figure (6-25) Gas liquid displacement inside domain F with no slip boundary conditions.....	133
Figure (6-26) Experimental pressure vs. detected diameters.....	135
Figure (6-27) Experimental results vs. analytically calculated data.....	136
Figure (6-28) Comparison of computed breakthrough pressures with experimental values, showing the effect of the calibration factor, for single pore with various pore diameters. ....	137
Figure (6-29) Pressure required to detect pores in single and multiple domains.....	138



## *Nomenclature*

---

$A$	Cross sectional area
$D$	Pores diameter
$f_a$	Relative number of pores
$f_d$	Relative flow through pores
$f_v$	Pore volume distribution
$J$	Water flux
$K$	Normalisation factor
$L$	Membrane thickness
$M_w$	Molecular weight
$N(d_p)$	Density of pore diameter ( $d_p$ )
$n_a$	Cumulative distribution of number of pores
$n_d$	Differential distribution of number of pores
$n_i$	Number of pores
$N_i$	Elemental shape function
$\hat{n}_x$	Unit vector in $x$ - direction
$\hat{n}_y$	Unit vector in $y$ - direction
$P$	Pressure
$P_0$	Initial pressure
$P_{atm}$	Atmospheric pressure
$R$	Gas constant
$r_k$	Kelvin radius
$T$	Temperature

$t$	Time
$T_b$	Absolute temperature
$T_{up}$	Upstream absolute temperature
$v$	Volume
$v_d$	Volumetric upstream gas loss
$v_x$	Velocity in $x$ - direction
$v_y$	Velocity in $y$ - direction

### **Greek Symbols**

$\eta$	Apparent viscosity
$\gamma$	Surface tension
$\theta$	Contact angle
$\Omega$	Solution domain
$\Omega_e$	An element domain within the solution domain
$\beta$	Slip coefficient
$\lambda$	Penalty parameter
$\mu$	Viscosity
$\Gamma$	Boundary of the solution domain
$\Gamma_e$	Boundary of an element domain
$\varepsilon$	Porosity
$\rho$	Density
$\tau$	Constriction tortuosity

## *Chapter 1 Introduction*

---

---

### **1.1. Preliminary Remarks**

Filtration is one of the well known conventional methods of physical separations applied in chemical and process engineering. It has broad applications industrially where the main objectives of applying it can either be clarification or liquor purification, separation of solid for recovery or improving other plant operations.

Filtration can be divided to many categories depending on the classification criteria. Membrane separation for example is one of these categories and has broad applications worldwide. Membrane separation processes are attractive for several reasons; the process is simple, there is no phase change involved which is measured in commercial applications as energy savings, the process is generally carried out at atmospheric conditions which besides being energy efficient, can be important for sensitive applications encountered in the pharmaceutical and food industries, and modules can be added and optimised in a process design flow sheet to achieve the desired separation

The filter medium is the main tool playing the active role in filtration applications, and for a perfect filtration process the filter medium should possess the following characteristics (Meltzer, 1987):

- The ability to retain a wide size distribution of solids from the suspension.
- Offer minimum hydraulic resistance to the filtrate flow.
- Allow easy discharge of cake.

- High resistance to chemical attack.
- Resist swelling when in contact with filtrate and washing liquid.
- Display good heat resistance within the temperature ranges of filtration.
- Have sufficient strength to withstand filtering pressure and mechanical wear.
- Capable of avoiding wedging of particles into its pores.

Membrane processes have enormous industrial applications as well. For any of these applications, and before using any membrane, the obvious first test is to characterise the membrane and thus define its operational capabilities and suitability for obtaining the required results. This characterisation requires defining the limits within which the membrane is capable of acting as a perfect barrier, consequently achieving the objectives of its installation. Different parameters are to be measured during the characterisation tests such as the pore size, the pore size distribution, mean flow pore size, bubble point, and others which will be discussed in more details in this thesis.

On the other hand, the hydrodynamics of the materials flowing through the membrane pores have been a fertile subject for investigations for some time. The development of computer modelling and simulation techniques enabled researchers to look at both the macro and microscale on what is happening within the filtration systems. The knowledge gained from this study provides us with comprehensive understanding on how materials behave; such knowledge helps to enhance the performance of the process.

There are many mathematical methods used for studying the microhydrodynamics within pores; use of the Finite Element Method (FEM) is widespread due to its flexibility and capability in dealing with complex geometries. The simulation of two phase flows increases the complexity of these engineering problems. To overcome such obstacles several mathematical techniques were developed, among these techniques the Volume of Fluid Method. The introduction of this method into the hydrodynamical equations enables monitoring the gas-liquid displacement occurring within the membranes at a microscale. The knowledge provided from how the gas and liquid interacts is used in this research, and compared to experimental data to provide a strong mathematical tool capable of relating the pore diameter for different membrane samples to the pressure required to detect these pores within a wet membrane. In other words, it provides us with the capability of simulating the bubble point test used in membrane characterisation and integrity monitoring.

## **1.2. Research Objectives and Practical Significance**

This research covers major two aspects. The first aim is an experimental investigations to characterise different membrane samples using the bubble point test. This test was carried out using Coulter II and PMI porometers. The objectives of the experimental tests were to detect the maximum pore diameter, the mean pore diameter, the minimum pore diameter, and the pore size distribution for different track etched membranes samples with manufacturers pore sizes ranging from 0.2  $\mu\text{m}$  to 12 $\mu\text{m}$ . The results obtained by both porometers were compared, the performance of each porometers was assessed.

The second aspect is to develop a computer program capable of solving the governing equations for fluid hydrodynamics occurring within the membrane pores as well as

the gas-liquid displacement. The Penalty scheme finite element method was used due to its suitability for simulating the boundary conditions applied experimentally. The velocity and pressure profiles inside different pore layouts were examined. The gas-liquid displacement occurring within the pore was simulated by the use of the volume of fluid method. This method provides us with the opportunity to monitor the interfacial boundary between the gas and the liquid, and thus monitor the gas liquid displacement occurring with the pore. From the simulation, a relationship involving the applied pressure required to detect a specific pore diameter will be established. The results obtained experimentally for different pore diameters were then compared with the simulation data to validate the capability of the developed program to detect the bubble point for different pore diameters.

### **1.3. Thesis Structure**

This thesis consists of seven chapters. Chapter 1 is an introductory about the research conducted and gives an infrastructure to the thesis by presenting a general view about the motivation behind this project, the objectives investigated as well as the methodology applied to conduct the work carried.

Chapter 2 presents a literature review and some of the work done in this field by other researchers within the last decade. It reflects on the different methods applied to membrane characterisation and carries a brief description behind each method, its principles, applicability, advantages and disadvantages.

Chapter 3 is the experimental procedure within which a description of the methodology is demonstrated. In this chapter the principles of the Bubble Point Test

is clearly presented. The chapter also shows how the mathematics behind porometry and what the results obtained provide us with.

In Chapter 4 a review of the simulation work done is presented. The method used for simulations is discussed and the techniques applied are demonstrated. The governing equations embedded in the computer program are explained and a description of how the model works is examined.

Chapter 5 discusses the results obtained experimentally using different types of porometers and a comparison between the experimental data the membrane manufacturer ratings.

Chapter 6 presents the results generated from the developed computer program on different domains. It also compares the experimental and numerical results as an approach to validating the developed computer program.

Chapter 7 is the conclusion of the work done and presented in this thesis. It shows the outcome obtained from both the experimental work and the simulation results beside the comparison carried between them and presented in Chapters 5 and 6. Recommendations for further work that needs to be carried for future validations are presented in the second section of Chapter 7.

## *Chapter 2 Literature Review*

---

### **2.1. Microfiltration**

Microfiltration can be defined as the separation of particles of one size from particles of another size in the range of approximately 0.01  $\mu\text{m}$  to 20  $\mu\text{m}$ . The fluid may be either a liquid or a gas. Microfiltration media are available in a wide variety of materials and from a variety of methods of manufacture. They can be rated either "absolute" or "nominal" depending upon the percentage of capture of particles of a particular size.

Membrane filters are generally rated as absolute media, (Ward *et al.* 1996). They can be manufactured of various polymeric materials, metals and ceramics. Nominal media include filters made of glass fibres, polymeric fibres, discrete particles, ceramics, etc. However, even absolute media can be considered absolute only in a finite time span because of the possibility of bacterial growth within their structure.

### **2.2. Membrane types**

Microfiltration membranes can be divided into two broad groups based on their pore structure, (Cheremisinoff, 1995). These are membranes with capillary-type pores manufactured by a track etching of pores, and membranes with tortuous-type pores or depth membranes.

#### **2.2.1. Depth membrane filter**

Figure (1) is a scanning electron micrograph of the surface of a typical depth, or tortuous pore, membrane. This membrane has a relatively rough surface where there appears to be many openings considerably larger than the rated pore size. Depth membranes nevertheless can be absolute, depending upon the random tortuosity of



their numerous flow paths to achieve their pore-size rating (Meltzer, 1987). Depth membranes are commercially available in pure silver, PVC, PVDF, PTFE, various cellulosic compounds, nylon, polyethersulfone, polypropylene, and many other materials.

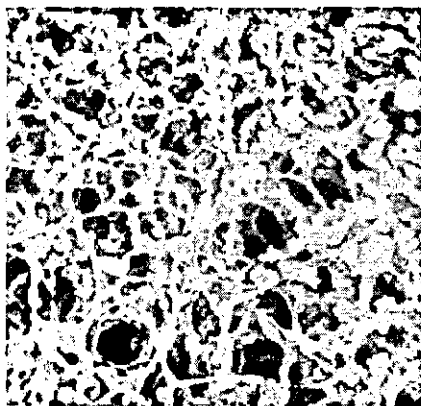


*Figure (2-1) Depth membrane filters.*

#### **2.2.1.1. Depth membrane production**

Most depth membranes are manufactured of various polymeric materials using a casting machine. Membranes cast with cellulosic esters are the most widely used membranes. Referring to Figure (2-2), cellulosic membranes are manufactured by dissolving the cellulose esters in a mixture of organic solvents; adding various chemical agents for improved characteristics; and casting the solution as a film approximately 150  $\mu\text{m}$  thick onto a moving belt. As solvents are evaporated under controlled conditions, the tortuous pore structure is formed. The resulting open area indicates high porosity ranges from 75% to 89%.

Membranes of this highly porous structure, with their labyrinth of interconnecting isotropic pores, are recommended for general precision filtrations, electrophoresis, sterilization of fluids, culturing of microorganisms and for many other larger scale uses.

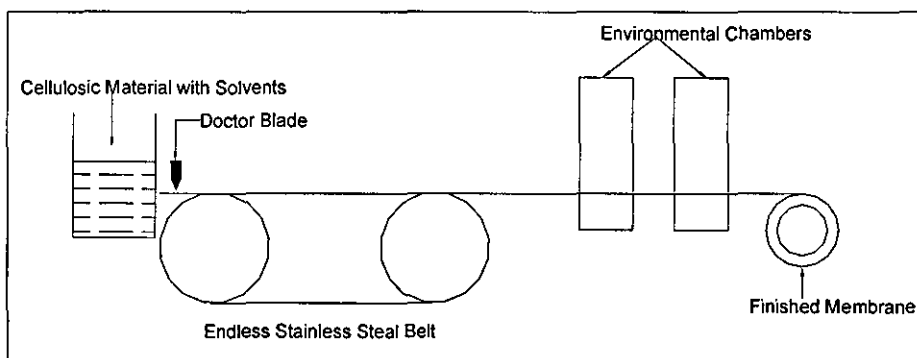


**Figure (2-2) Depth membrane production**

Another example is the PTFE (polytetrafluoroethylene) depth membranes which are manufactured by the controlled stretching of a fluorocarbon sheet. Some polypropylene membranes have also been manufactured by this method. On the other hand, silver membranes are manufactured of pure metallic silver particles that are molecularly bonded to each other to form a uniform porous monolithic structure. A major application for silver membranes is inorganic material analyses. These are some of the methods used for different depth membrane manufacturing processes.

### **2.2.2. Track-etched membranes**

Figure (2-3) shows a scanning electron micrograph of the surface of a track etched, or capillary pore, membrane. This membrane has nearly perfect cylindrical pores, more or less normal to the surface of the membrane, with a random pore dispersion over the surface.

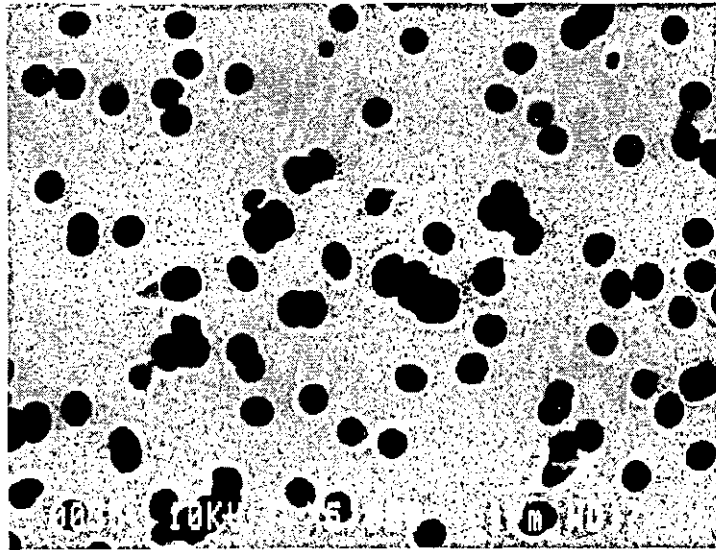


*Figure (2-3) Track etched membrane*

Track etched membranes are absolute and are commercially available in thin films of polycarbonate and polyester. They are manufactured in a two steps; nuclear track and etch process. They are preferred in a wide variety of applications including optical and electron microscopy, chemotaxis, exfoliative cytology, particulate analyses, aerosol analyses, gravimetric analyses and blood rheology but they are not appropriate for larger scale process applications.

Track etched membranes are prepared in the laboratory by exposing commercially available polycarbonate sheets of about 6 mm thickness to alpha particles emitted from nuclear reaction followed by chemical etching (Ferain and Legras, 1997). A series of membranes can be produced using different bombardment and etching, periods and the hydraulic conductivity of the resulting porous membranes can be measured for applied pressures from 10 to 50 kPa. They also possess very low porosity ranging from 5 to 12%.

### 2.2.2.1. Track etched membrane production

Two steps are considered in the production of track etched membranes:

- In the first step, thin plastic film is exposed to ionising radiation forming damage tracks.
- In the second step, the tracks are preferentially etched out into pores by a strong alkaline solution as presented in Figure (2-4).

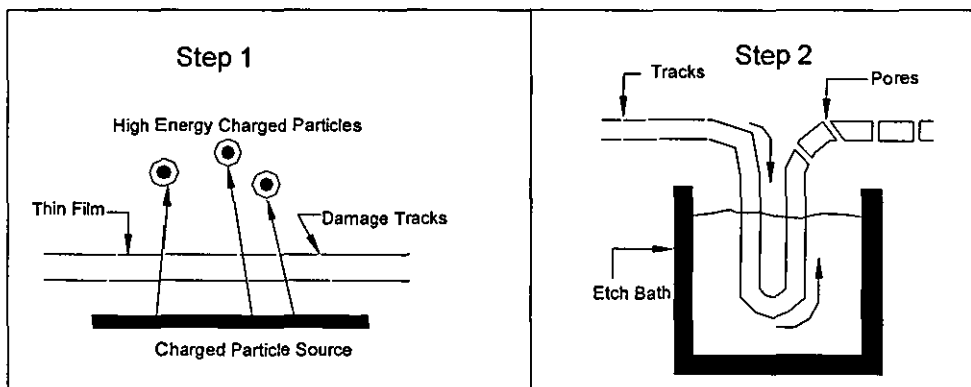


*Figure (2-4) Track etched membrane production*

### 2.3. Pores

Pore size can have a great influence on the rate of penetration of the liquid through the membrane. It controls the flow pattern of a liquid flowing through a porous material or how a collection of particulates will be captured by a filter. It is responsible for the uniform or non-uniform distribution of the liquid within a porous network or between two or more adjacent networks.

Pore structure of filtration media can be complex from the geometric point of view. It can be formed from different regular or irregular shapes. Generally there are many types of pores: *Blind pores* terminate inside the filtration medium and do not permit

the fluid to flow, but blind pore surface area can absorb gases, capture small particles and participate in reactions (Jena and Gupta, 1999). *Closed pores* are not accessible and do not play an active role in the filtration process. Our main interest in this research is the pores described as the *Through pores*, extending from one side of the filter medium to the other and permitting fluid flow. Figure (2-5) presents schematic of the different types of pores explained.

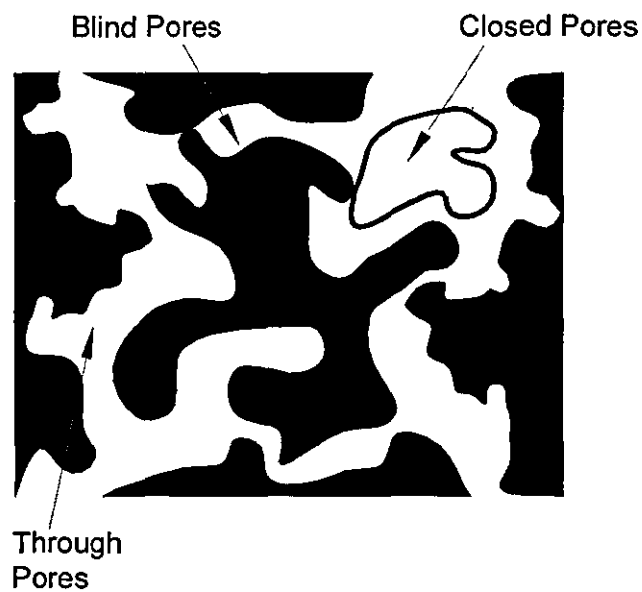


**Figure (2-5) Types of pores**

Another important factor governing the separation capabilities of microfiltration membranes is the pore size distribution. Two membranes can have the same pore size or the same molecular cut-off value yet have quite different separation characteristics when there is a difference in the pore size distribution in the membrane (Ames *et al.* 2003). Therefore, in order to accurately predict the separation capabilities of a given membrane, an understanding of a pore size distribution is necessary.

The size of the particles that cannot pass through filtration media is determined by the size of the pores at their most constricted parts. Therefore the largest, the mean and the range of the most constricted through pores size, the shape of the pore and the pores distributions are the most important characteristics determining the barrier capabilities of the filtration medium.

#### **2.4. The characterisation of porous membranes**

Characterisation data for porous membranes often gives rise to misunderstanding and misinterpretations. It is not unreasonable that it is mainly the size of the pores in these membranes that determine which solute can pass or which will be retained.

Generally we are looking for the pore size and the pore size distribution, but in actual separation processes the membrane performance is governed by other factors such as concentration polarisation and fouling. Another important factor is the shape of the pore or its geometry; due to the complexity of combining the geometrical aspects to physical equations, to simplify the problem assumptions are made for standard geometries of pores. This limits most of the modelling applications governing these processes, nevertheless the use of track etched membranes (such as Nuclepore membranes as in this project) most nearly meets this assumption due to the nature of how the pores are manufactured.

In general, the pores in microfiltration membranes are not monosized but exist as a distribution of sizes, and for that reason the pore size distribution is another important factor to be examined. The surface porosity is also a very important variable in determining the flux through the membrane in combination with the thickness of the membrane or the length of the through pores.

Different tests can be conducted to determine these parameters; for example, the bubble point test determines the maximum pore size of the membrane. The capillary

flow test determines the mean flow pore size, bubble point, cumulative flow, and pore size distribution. This project will focus on the capillary flow porometers and their application in defining these parameters. Nevertheless, there are several independent techniques for determining pore statistics. These are summarised by Hernandez *et al.* (1996).

#### 2.4.1. Mercury porosimetry

This method is based on the variation of the bubble pressure method when mercury is used to fill a dry membrane and can be used to measure blind pores as well as through pores. Mercury is a non-wetting liquid for most materials. For a non-wetting liquid, the surface tension between the solid/gas ( $\gamma_{\text{solid/gas}}$ ) is usually less than that between the solid liquid ( $\gamma_{\text{solid/gas}} < \gamma_{\text{solid/liquid}}$ ), therefore, such liquid cannot spontaneously flow into the material pores (Salmas and Androutsopoulos, 2001). Mercury can be forced into pores by applying pressure. Equating the work done due to forcing mercury into a pore to the increase in surface free energy and using the definition of pore diameter:

$$p = \frac{-4\gamma \cos \theta}{D} \quad (2-1)$$

where  $p$  is the applied pressure,  $D$  is the pore diameter,  $\theta$  is the contact angle and  $\gamma$  is the surface tension. From this equation, the measured differential pressure yields the pore diameter. The volume of intruded mercury gives the pore volume. In this technique, as mercury at a given pressure intrudes a certain part of a pore, the diameter of that part of a pore is obtained from the pressure. On the other hand, the pore volume distribution is given by the distribution function:

$$f_v = -\frac{dv}{d \log D} \quad (2-2)$$

where  $v$  is the volume and  $D$  is the pore diameter. The function is such that the area under the distribution in any pore diameter range yields the volume of the pores in that range.

The main drawback of this technology is that membrane structure is distorted due to the high pressure needed to analyse small pores. Another disadvantage is that it is a destructive method of analysis given that some mercury remains trapped within some pores.

#### **2.4.2. Thermoporometry**

Hernandez *et al.* (1996) suggested thermoporometry to analyse the pore distribution on the basis of the fact that the solidification point of the vapour condensed in pores is a function of the interface curvature. A differential scanning calorimeter monitors the phase transition from which the pore distribution can be calculated. Mulder (1991) stated that thermoporometry is based on the calorimetric measurement of a solid-liquid transition (e.g. of pure water) in a porous material. This can occur in pores in the skin of an asymmetric membrane, the temperature at which the water in the membrane freezes depends on the pore size. As the pore size decreases the freezing point of water decreases. Each pore size has its own freezing point. The major drawback of this technique is that all pores present in the membrane, in the sub-layer as well as in the top layer, are characterised, including dead-end pores which make no contribution towards transport, hence one is unable to distinguish between them.

#### **2.4.3. Permporometry**

Mietton-Peuchot *et al.* (1997) applied the permporometry characterisation technique to determine the pore size distribution of active pores in a membrane, as such a



technique outlines a method of choosing an appropriate microfiltration membrane. Liquid-gas porometry allows the measurement of membrane characteristics for pore sizes ranging from 0.07 to several hundred microns. Permporometry is based on controlled blocking of pores by condensation of vapour, present as a component of a gas mixture and simultaneous measurement of the gas flux through the membrane. Using the Kelvin equation presented by Nakao (1994) in the formula:

$$RT \ln \frac{p}{p_o} = \frac{2\gamma V \cos \theta}{r_k} \quad (2-3)$$

where  $p$  and  $p_o$  are the vapour pressure in the capillary and under standard conditions, respectively,  $\gamma$  is the surface tension between the capillary liquid and air,  $V$  is the molar volume of the liquid,  $\theta$  is the contact angle,  $r_k$  the Kelvin radius,  $R$  the gas constant, and  $T$  the absolute temperature. Nakao (1994) stated that the actual pore radius is a little larger than the Kelvin radius calculated from equation (2-3) as an adsorbed layer of the condensate gas makes this different and that the vapour pressure of the liquid in a capillary increases as the radius of the capillary increases.

On the other hand, capillary condensation provides the possibility of blocking certain pore sizes with liquid, just by setting the relative pressure. This principle is combined with the measurement of the free diffusive transport through open pores. Starting from a relatively low pressure all pores of the membrane are filled so that unhindered gas transport is not possible. When the pressure is reduced, pores having a size corresponding to the vapour pressure are emptied and become available for gas transport. Measuring the gas flow through the membrane upon decreasing the relative pressure, the distribution of the size of the active pores can be found. Although similar measurements can be carried on during adsorption process, Nakao (1994)) stated that

it is more difficult to reach the equilibrium and therefore quantitative analysis of the desorption process is preferred.

Mulder (1991) stated that by using this method in asymmetric membranes where transport is determined by the top thin layer, information can be obtained about pore size and pore size distribution of the active pores in the top layer. On the other hand using permoporometry for pore size determination is not accurate because it does not consider the pore area available for transport when there are narrow pore openings or other irregularities in pore shape.

#### **2.4.4. NMR measurements**

Hernandez *et al.* (1996) referred to the studies by previous researchers demonstrating the determination of pore size in water-saturated membranes using Nuclear Magnetic Resonance (NMR) spin lattice relaxation measurements. The strength of the local magnetic field acting on a given nuclear spin in matter is slightly different from that of the external field (Nakao, 1994). The electron cloud surrounding a nucleus induces a shield effect, shifting the observed resonance lines. This is known as the chemical shift, which for the NMR comes from such interactions. The highly sensitive chemical shift of NMR has contributed to the elucidation of complex organic molecular structures. The cause for the chemical shift is not necessarily in the molecule, but in the surroundings. In particular, molecules in a confined solid space such as a micropore or a mesopore are affected by the electronic states of the surroundings.

#### **2.4.5. Light transmission method**

This method was used by Ju Youn *et al.* (1998) and uses the transmissivity of light from a transparent liquid filling of the pores of an opaque membrane. It was found that the change of light transmissivity is proportional to the volumes of the pores

filled with the liquid, and the distribution of the pore size can be determined by combining this phenomenon with the bubble pressure method. The Light Transmission Method (LTM) is one of the new techniques and is still under investigations as few researches are reported to use this method.

#### **2.4.6. Scanning electron microscopy (SEM)**

This is one of the techniques that can be used for membrane characterisation (Reutov *et al.* 2003, Mulder, 1991). Two basic methods can be distinguished: scanning electron microscopy (SEM) and transmission electron microscopy (TEM); of these two methods SEM provides a very convenient method for investigating porous structure for microfiltration membranes. The principle of this method is to hit the membrane coated with conducting layer, usually gold, by a narrow beam of primary (high-energy) electrons. Secondary electrons (low-energy) are then liberated from atoms in the surface determining the image presented in a screen of the micrograph. High resolution scanning electron microscopy has been used in a number of studies to determine pore size characteristics in various micro- and ultrafiltration membranes, however, samples must be coated with a conducting metallic film and therefore the actual pore size can be larger than those observed. Also, for some materials the pore sizes observed under dry conditions necessary for SEM may be different from the pore sizes presented when the membrane is exposed to a solvent, and it is clear from the description of the process that it is a destructive test.

#### **2.4.7. Atomic force microscopy (AFM)**

This test has also been used in pore characterisation. The metallic coating which is applied in the SEM is not required in this case but AFM images are distorted by complexity between pore shape and cantilever tip shape and therefore the quantitative

determination of pore size from an AFM image is not always straightforward (Boccaccio *et al.* 2002).

In addition both the SEM and AFM can only give information about the characteristics of the membrane surface which may be different than the sub-surface characteristics and may not truly reflect the separation capabilities of the membrane.

#### **2.4.8. Permeability method**

If capillary pores are assumed to be present, the pore size can be obtained by measuring the flux of a fluid through a membrane at a constant pressure using the Hagen-Poiseuille equation:

$$J = \frac{\varepsilon r^2}{8\eta\tau} \frac{\Delta P}{\Delta x} \quad (2-4)$$

where  $J$  is the water flux through the membrane at a driving pressure gradient of  $\Delta P / \Delta x$ , with  $\Delta P$  being the pressure difference and  $\Delta x$  the membrane thickness. The proportionality factor contains the pore radius  $r$ , the liquid viscosity  $\eta$ , the porosity of the membrane  $\varepsilon$ , and the tortuosity factor  $\tau$ .

The use of both the bubble point method and the permeability method can then be applied to calculate the pore size distribution at various operating pressures.

#### **2.4.9. Gas adsorption-desorption**

Analysis of pore size distribution by gas adsorption/ desorption is based on the Kelvin equation, which relates the reduced vapour pressure of a liquid from a plane surface. Also, application of BET adsorption isotherms is commonly used to obtain specific surface areas.

This is one of the latest methods applied for pore size measurements. The absorption isotherm of an inert gas is determined as a function of the relative pressure. Nitrogen is the most common gas applied in this method. The method is usually carried out at liquid nitrogen boiling temperature at a pressure of 1 bar.

#### **2.4.10. Bubble pressure breakthrough**

There has been a considerable amount of effort directed towards developing methods of determining pore size and its distribution in porous membranes. This method is one of the most applied for this purpose and is based on the measurement of the pressure necessary to blow air through a water-filled porous membrane.

Interpretation of results using this method requires knowledge of the contact angle between the liquid, vapour and membrane materials. Uncertainties in the contact angle between the membrane and the two fluids can introduce problems when interpreting the results (Baltus, 1997).

There are different types of porometers that use this method for membrane characterisation, for examples the Coulter II porometer uses a liquid displacement technique where the sample is first wetted with a wetting liquid (e.g. Porofil or Galwick) of a low surface tension, low vapour pressure, and low reactivity. The wetting liquid fills the pores since it has zero contact angle with many materials; this method has been used by many researchers (Calvo *et al.* 1995). The use of low surface tension liquids is a must as hydrophobic filters, by their nature, resist being penetrated by water. Such wetting can be induced by the imposition of a pressure sufficient to force water into the membrane pores (Meltzer, 1987). The wetted sample is subjected to increasing pressure up to 14 bar, applied by compressed, clean, and dry air source, at ambient temperature.

As the pressure of the air increases, it will displace the liquid from the pores of diameter given by the equation:

$$r = \frac{2\gamma \cos \theta}{\Delta P} \quad (2-5)$$

where  $r$  is the pore diameter,  $\Delta P$  is the pressure drop,  $\theta$  is the liquid contact angle and  $\gamma$  is the surface tension.

#### **2.4.11. Glass bead challenge test**

Whitehouse Scientific Ltd. established a new method for direct measurement of pore size by the use of narrow size distribution microspheres (Rideal, 2006). This is achieved by accurately measuring the particle size distribution both by microscopy and a precision sieving method, which helps construct a calibrator graph for the microspheres where the percentage of the beads passing an unknown mesh can be used to calculate the filter cut point. The company produces a range of 20 filter calibration microspheres for calibrating meshes from 20  $\mu\text{m}$  to 700  $\mu\text{m}$ . This method simply depends on high frequency mechanical shaking of the membrane after covering it with the microspheres, the shaking ensures transport of the beads through the membrane and overcomes the possibility of the beads being lodged in dead end pores. Several meshes were tested using this method and gave precise filter cut point (Rideal, 2006). This is one of the major advantages of this method as the cut point describes the pore sizes in a filter required to remove all the particles from the liquid suspension.

The limitation of this method comes from its validity to deal with meshes and membranes having straight pores. The presence of blind and dead end pores imposes problems as they cannot be evaluated using this method. Another limitation is the

interaction forces between the beads, specially at diameters less than 20  $\mu\text{m}$  (Rideal, 2006).

Although methods of characterisation of porous media such as nitrogen adsorption-desorption and mercury penetration are well known and widely accepted, such methods are unsatisfactory for some types of membranes, for example asymmetric ceramic membranes. Mercury penetration studies employ high pressure and cannot distinguish between dead-end pores and pores available for permeation. Nitrogen absorption-desorption detects very small pores, but cannot distinguish dead-end pores. Also, most methods are unable to differentiate between the thin active separation layer of interest and the pore support. Although the active layer determines the filtration performance, it typically constitutes only a very small fraction of the porous material in a membrane (Jakobs and Koros, 1997). Due to the large difference in pore size and pore volume of the active layer and the support, characterisation of the selective layer typically lacks detail and resolution. Finally both, the nitrogen adsorption-desorption and mercury intrusion methods are based on artificial and simple models of the porous structure e.g. straight, cylindrical, non-intersecting pores of uniform and invariable radii (Jakobs and Koros, 1997).

Membrane selection is still subject to empirical data and should be made only after numerous pilot tests. Mietton-Peuchot *et al.* (1997) were able to measure pore size distributions for both clean and fouled membranes using liquid permoporometry and thus were able to develop a methodology for choosing membranes appropriate to microfiltration.

## 2.5. Measuring the pore size distribution

Liquid porometry allows measurement of membrane characteristics for pore sizes ranging from 0.07 to several hundred microns (Troger *et al.* 1998). The principle of this process is based on the notion of capillary pressure, as represented by equation (2-5).

To replace a fluid which is saturating the pore of the membrane with another fluid which is less wetting, one must apply a pressure of  $\Delta P$ , being greater than the capillary pressure generated by the radius of the pores.

Determination of pore size distribution in membranes by monitoring liquid permeation has been used for many years (Jakobs and Koros, 1997). Like the previously mentioned approach these methods have their drawbacks as well. No uniform nomenclature exists, and various names are used for related tests, such as Coulter porosimetry, bubble point test, permoporometry, biliquid permoporometry and thermoporometry, just to name a few. In fact, the above mentioned methods are rather similar and rely on the same basic physical principle, the displacement of a wetting liquid (Jakobs and Koros, 1997).

### 2.5.1. Porometer theory

The porometer is based on the principles of capillary rise. When a capillary tube is immersed in a liquid, because of the surface tension of the liquid, the liquid is drawn up the capillary until equilibrium is established with the force of gravity. The equilibrium condition is expressed by the Washburn equation

$$rP = 2\gamma \cos \theta \tag{2-6}$$

where  $P$  is the pressure,  $r$  radius of capillary or pore,  $\theta$  is the contact angle between the liquid and capillary wall and  $\gamma$  is the surface tension of the liquid.



If the liquid completely wets the capillary it has zero contact angle, therefore  $\cos \theta = 1$  and the equation become:

$$r = \frac{\gamma}{P} \quad (2-7)$$

The porometer monitors both pressure and flow and records these in a pressure versus flow graph for wet and dry samples. The dry data curves are determined after all the liquid has been expelled from the pores. This dry curve becomes the reference for calculating the pore distribution. A percent flow distribution is calculated from the difference between wet and dry curves. If the flow is proportional to the pore area, the flow distribution can be described in terms of the pore area percent (Jena and Gupta, 2002 and 2001). If we assume constant pore length, then the area distribution data will be equivalent to those of the volume distribution. Taking the square root of the area/volume values, we obtain the number distribution. Mean flow pore size (MFP) is calculated from the pressure at which the wet flow is half of the dry flow. The maximum and the minimum pore sizes are determined from the bubble point and from the point where wet and dry curves converge.

## 2.6. Membrane integrity

Low pressure membrane filtration processes, including UF and MF have been well established as powerful disinfection and clarification processes with a diverse application potential in many industries including water purification.

Contaminant removal in UF and MF is essentially characterised by a physical sieving process. The pore size of MF and UF membranes is small enough to make absolute removal of protozoa, including *Giardia* and *Cryptosporidium*, possible (Edwards *et al.* 2001). It was proven from previous researchers that MF and UF can provide a total barrier for these protozoa (Crozes *et al.* 2002), when the integrity of the membrane is

not compromised. Thus, absolute removal of these contaminants assumes that the integrity remains intact. In practice, the integrity may be compromised due to different types of leakages that could develop in the membrane. For example these could include a breach, chemical degradation, or biological degradation of the membrane, or mechanical failure of O-rings, gaskets, potting or glued fittings. Membrane integrity tests performed to date have typically involved pilot-scale tests. However, microbial removal cannot be guaranteed based on those tests because the sensitivity based on the integrity monitoring method decreases with the size of a membrane investigated.

There are number of reasons why a membrane integrity test is performed. These can be summarised in the following:

- ✓ Operational plant routine control and checking
- ✓ Monitoring performance
- ✓ Following integrity failure and repair
- ✓ Operational plant special case
- ✓ Commissioning new plant or new membranes
- ✓ Following periods of shut down
- ✓ Specific performance analysis
- ✓ Pilot plant testing
- ✓ Quality control.

Monitoring membrane integrity can be considered with the intensions of monitoring the membrane system of a plant. Also, monitoring the membrane integrity can be performed for quality control purposes during its manufacture, and by this the membrane itself (rather than the entire membrane module) is under scrutiny. Although

both methods measure the same parameters, bubble point, pore size distribution etc, but the size and the interpretations of the results of the test are completely different.

### **2.6.1. Methods of measuring membrane integrity**

Membrane integrity tests can be classified as direct or indirect.

Direct methods include the pressure decay test and online sonic testing. Indirect monitoring methods include particle counting at various sensitivities, index based particle monitoring, count based particle monitoring, turbidity monitoring, laser turbidity monitoring, multi-sensor laser turbidity monitoring.

Amongst the direct methods, the pressure decay test (PDT) is the most frequently used method and is employed at almost all plants (Nederlof *et al.* 1997). The other direct methods, the bubble point test and manual sonic testing, are employed at some industrial plants as “secondary methods”. That is, these methods are employed to locate the location of a breach, after the response from a primary method (typically the PDT) has indicated a potential integrity failure. It is noted that while the PDT offers high sensitivity as a direct integrity monitoring method, it results in contributing to plant downtime.

Of the indirect methods, turbidity monitoring and routine microbial analysis are used most frequently (Edwards *et al.* 2001). However, it is noted that turbidity monitoring does not provide the desired sensitivity to detect membrane breaches at full scale while routine microbial analysis is not an online method and it is time consuming. Particle counting, though sometimes considered to be relatively costly, is the next most popular method and is utilised by great number of plants.

Monitoring of membrane integrity is necessary to ensure that an adequate barrier is provided continuously by the membrane during the separation process. Damaged filters may have an impact to some extent on the treated filtrate quality; thus

membrane integrity control is a must to ensure high process performance. The various monitoring techniques summarised above are discussed in more detail as well as the different parameters affecting the performance of these tests.

#### **2.6.1.1. Direct integrity tests**

These tests directly measure a breach in a membrane or membrane system. Direct tests monitor gas passing through a breach, filtrate flow rates, pressure or sound changes or any other detectable variations.

##### **2.6.1.1.1. Air pressure decay testing (PDT)**

In this test the membrane is pressurised to approximately 70-80% of the bubble point pressure. This test involves applying pressurised air to the feed side to a pre-determined level below the bubble point and then isolating the feed side. The pre-determined pressure directly relates to the size of defects under investigation. The air pressure is monitored for a period of time (2 to 10 minutes depending on the size of the membrane sample under investigation) to observe the rate of decay (Farahbakhsh and Smith, 2004). A small decrease of 0.1 or 0.2 psi per minute is considered acceptable and is due to diffusion of the air across the microporous membrane structure. A faster decrease in pressure indicates a faulty membrane. As the membrane system is open to atmospheric pressure on the filtrate side, the airflow can be observed to confirm the location of any breach. Minimal loss of the hold pressure at the filtrate side after a period of time indicates a passed test, while a significant decrease of the hold pressure indicates a failed test.

This method is capable of detecting changes in the integrity at levels up to 4.5-5 log reduction value (LRV). The log reduction scale stands for a 10-fold, or one decimal,

or 90% reduction in numbers of recoverable bacteria in a test. Table (2-1) demonstrates an understanding for log reduction numbering.

Log reduction	% Reduction of Bacteria
1	90
2	99
3	99.9
4	99.99
5	99.999

Table (2-1) Log reduction chart

Hofmann (1984) stated that the gas loss through a pressurised filter assembly caused by diffusion or viscous flow can be determined either by measuring the gas with volumetric methods downstream of the membrane or by determining the pressure loss at the upstream side when the pressure supply valve of the system is closed. The upstream pressure loss caused by a corresponding gas loss and can be calculated from the equation:

$$\Delta p = \frac{V_d P_{atm} T_{up}}{V_{up} T_b} \tag{2-8}$$

where  $\Delta p$  is the upstream pressure loss,  $P_{atm}$  the atmospheric pressure,  $T_b$  is the absolute temperature,  $V_d$  the upstream gas loss volumetrically determined downstream of the membrane,  $V_{up}$  is the volume of filter system upstream of the membrane and  $T_{up}$  is the absolute temperature of the filter assembly upstream of the membrane.

Equation (2-8) shows that the upstream pressure loss not only depends on the upstream gas loss but also on the upstream volume of the filter system. Therefore, it is not possible to arrive at a decision to accept or reject a filter element in terms of

pressure loss per unit time without taking into account the volume of the filter system and a known expected value of permeability of a filter. The positive feature of the pressure hold test is that it is non-invasive of the downstream side of the membrane under investigation and that it is employed in initial integrity testing, and that it is measurable using sensitive devices. Its shortcoming is its insensitivity at low pressure readings.

#### 2.6.1.1.2. Diffusive air flow test

The diffusive air flow test uses the same concepts as the PDT or air pressure hold test, but is performed by monitoring the displaced liquid volume due to the air leaking from a compromised membrane in accordance with the physical law governing the solubility of gases in liquids. More air is dissolved at the higher pressure present at the upstream portion of the thin water layer wetting the filter than in the downstream portions. This is due to Henry's law, which states that the amount of a gas dissolved in a liquid is directly related to the gas pressure over the liquid. As a result, as the dissolved gas (forced into solution by higher pressure) diffuses to the downstream lower pressure region of the water layer. The amount of air that diffuses out on the downstream side of the membrane can be detected as bubbles before the bubble point is reached. This test is more sensitive than the air pressure hold test because it is technically easier and more accurate to measure small variations in liquid volume rather than small variations in air pressure. This test is fundamentally similar to the pressure decay test (PDT) but is capable of detecting integrity changes at levels more than 6 LRV.

#### 2.6.1.1.3. Bubble point test

Bubble point testing can identify the membrane or seal location that is compromised in a membrane module. This test is typically performed after the compromised module has been identified by a sonic sensor or other monitoring method. After identifying the compromised membrane, it can be isolated from the module for recovery. Although the bubble point is a common test for measuring the integrity of a membrane, its main drawback is its dependence on the sensitivity of the observer in detecting the bubble point (Johnson *et al.* 1981). This major fault was overcome by the application of high sensitive electronic sensors.

#### 2.6.1.2. Indirect integrity monitoring tests

This method of monitoring membrane integrity includes those that do not evaluate the membrane itself, but rather use a surrogate parameter for assessing the membrane's condition.

##### 2.6.1.2.1. Turbidity monitoring or reduction monitoring

In this method the turbidity of the feed water and the filtrate are monitored. An intact membrane would be expected to show a considerable reduction in turbidity from feed to filtrate. If the feed waters were relatively clean, the differences in measurement can be beyond the resolution capabilities of turbidity meters.

##### 2.6.1.2.2. Laser turbidity test

Similar to the above test, but measurement of the diffraction of a laser beam from the permeate is used (Ju Youn *et al.* 1998).

##### 2.6.1.2.3. Particle counters

A particle counter can count and monitor different sizes of particles in the filtrate. If the feed waters were relatively clean, differences in measurement would be beyond

the limits of current particle counters. Panglisch *et al.* (1998) examined the integrity of a capillary membrane using the particle counting method in a pilot plant and concluded from that particle counting is much more sensitive than turbidity monitoring.

#### 2.6.1.2.4. Conductivity tests

This test can be applied when the membrane removes significant amounts of dissolved ionic species. The product and feed waters will then have different ionic strength/conductivities. A defective membrane system will pass more ionic species; the conductivity instruments can identify such occurrences on-line. This test is therefore only relevant for reverse osmosis and nanofiltration membrane types. Adham *et al.* (1998) examined the integrity of RO using both particle monitoring and conductivity tests and concluded that the on-line particle counting was not sensitive enough to detect a minor compromising condition at relatively low particle concentration, whereas the on-line conductivity succeeded.

Generally, direct monitoring methods should be the most effective in identifying compromised membranes, but some of the techniques developed to date do not provide continuous monitoring of membrane integrity, and interruption of operation is necessary to conduct the test.

The air pressure hold test is convenient and reliable because it can be built into the membrane system for frequent evaluation of membrane integrity. The test concept is an integrity check of the membrane module and is thus very sensitive. The air pressure hold test can be applied to a whole rack of membrane modules simultaneously which is an advantage compared with other direct monitoring methods, which are more labour intensive. The other direct methods for monitoring



membrane integrity are the bubble point test and sonic sensors. They are important because the compromised module, or hollow fibre, needs to be identified and repaired before module reuse.

Indirect monitoring for membrane integrity through the use of on-line particle monitoring instruments has the advantage of providing continuous evaluation of membrane integrity. Table (2-2) summarises some integrity monitoring methods and compares between their advantages and disadvantages.

Monitoring method	Advantages	Disadvantages
Particle counting	Continuous on-line measurements, measures several size ranges	High cost, indirect measurement of membrane integrity, may require several sensors for large scale applications
Particle monitoring	Continuous on-line measurement, low cost	Does not count particle size ranges, may require several sensors for large scale applications
Turbidity monitoring	Extensive water industry applications, low cost	Not sensitive at low turbidity, indirect method for monitoring integrity
Air-pressure testing	Built into membrane system, direct measuring method of integrity	Not a continuous monitoring system
Bubble point testing	Direct monitoring method for integrity	Must be conducted manually, labour intensive for large plants

Table (2-2) Comparison of different integrity monitoring methods

## 2.7. Gas Capillary Flow

Membrane filtration processes are used industrially as an alternative to conventional separation methods. Membrane separation methods can be divided into classes according to their separation characteristics to the following criteria:

1. Separation by sieving action;
2. Separation due to a difference in affinity and diffusivity;
3. Separation due to difference in a charge of molecules; carrier-facilitated transport;
4. Process of (time-) controlled release by diffusion.

In all these cases diffusion processes play an important role in the transport mechanism of the solutes (van den Berg and Smolders, 1992). Various mechanisms have been distinguished to describe the transport in membranes: transport through bulk material (dense membranes), Knudsen diffusion in narrow pores, viscous flow in wide pores, or surface diffusion along pore walls. In practice, the transport can be a result of more than only one of these mechanisms. For all of these mechanisms models have been derived. The characteristics of a membrane can also have major consequences for the rate of diffusion in the membrane, and hence for the flux obtained.

There are other different models that were suggested by researchers (McGuire *et al.* 1995; Hernandez *et al.* 1996) that relate the volume flow of each pore diameter in the distribution to the viscosity of gas under the assumption of having a straight circular pores.

### 2.7.1. Hagen-Poiseuille Model

When the mean free path of the gas molecules is lower than the capillary diameter, the transport velocity at the capillary walls are set to zero. Using the basic equations of viscous flow, the volume flow for each pore diameter in the distribution is given by the Hagen-Poiseuille equation:

$$J_v(d_p) = \frac{\pi N(d_p) d_p^4 \Delta p}{128 \eta \psi \Delta x} \quad (2-9)$$

where  $d_p$  is the pore diameter,  $N(d_p)$  is the density of pore diameter  $d_p$ ;  $\psi$  is the constriction-tortuosity factor and  $\eta$  is the gas viscosity,  $p$  is the pressure applied,  $\Delta x$  is the membrane thickness and  $J_v$  is the volumetric flow rate.

### 2.7.2. Knudsen Model

When the pressure is small and the pore size is also lower than the mean free path of the gas molecules, the expression for the flow becomes more complex. In this situation the flow is referred to as free molecule diffusion or Knudsen flow. Considering the diffuse reflection of the gas molecules after their collision against the capillary wall the volume flow is expressed as:

$$J_v(d_p) = \frac{2\pi N(d_p)}{3} \left( \frac{RT}{8\pi M_w} \right)^{1/2} \frac{d_p^2 \Delta p}{p \psi \Delta x} \quad (2-10)$$

where  $M_w$  is the molecular weight of the gas and  $p$  is the downstream pressure.

### 2.7.3. Knudsen- Poiseuille Model

The Hagen-Poiseuille model holds true for the condition  $d_p \gg \lambda$  while Knudsen model gives the flow rate when  $\lambda \gg d_p$ . But when  $\lambda$  is smaller than  $d_p$  but not negligibly small the Poiseuille equation is used with an additive corrective term

representing the effect of slip at the surface of the pore. The corrected flow equation can be written as:

$$J_v(d_p) = \frac{\pi N(d_p) \Delta p}{\psi \Delta x} \left[ \frac{d_p^4}{128\eta} + \left( \frac{\pi RT}{8M_w} \right)^{1/2} \frac{d_p^3}{8p} \right] \quad (2-11)$$

Hernandez *et al.* (1996) examined the porous morphology of several track etched membranes using the bubble point method and concluded that equations (2-11), (2-12) and (2-13), when analysed for the particular values of  $T$ ,  $M_w$ ,  $\psi$  and  $\eta$  that the Hagen-Poiseuille flow was acceptable for capillary diameters over 0.96  $\mu\text{m}$ . For the capillary diameters below 0.96  $\mu\text{m}$ , reasonably good results were obtained by using Knudsen flow.

Following the method mentioned by McGuire *et al.* (1995), Martinez-Diez *et al.* (2000) characterized the filter medium with a discrete pore size distribution given by the equation:

$$\frac{n_j}{\Delta r_j} = \left[ \left( \frac{J_{j+1}}{\Delta p_{j+1}} \right) - \left( \frac{J_j}{p_j} \right) \right] \frac{8L\eta\psi}{\pi R_j^4 \Delta r_j} \quad (2-12)$$

where  $\Delta r_j = r_j - r_{j+1}$  and  $R_j = r_j - \Delta r_j/2$  while  $L$  is the membrane thickness and  $\Delta p$  is the applied transmembrane pressure drop,  $n_j$  is the number of pores,  $\eta$  is the viscosity,  $J_j$  is the flow obtained through a particular diameter  $j$  and  $R$  is the centre radius of a class in the discrete distribution (length).

It was found that the relative number of pores with radii between  $r_j$  and  $r_{j+1}$  can be found using the above equation. The absolute number of pores is not specified by the equation.

Similarly, the continuous pore size distribution was represented by the function:

$$f(r) = \left( \frac{dJ}{d(\Delta p)} - \frac{J}{\Delta p} \right) \frac{8\eta\psi L \Delta p^5}{\pi(2\gamma \cos\theta)^5} \quad (2-13)$$

The assumption made for the derivation of the above equation is that the membrane area is large enough so that the pore size distribution can be considered continuous.

In general, the transport can be considered to be mainly of the Knudsen diffusion type when the pore radius  $r$  is smaller than 10 nm at ambient pressures and it will be mainly viscous (Poiseuille) flow when  $r$  is larger than 10  $\mu\text{m}$ . These values also depend on the applied pressure and temperature. In between these pore sizes the flow is a combination of Knudsen and Poiseuille flow and the performance of the membrane is determined mainly by its pore size and the nature of the membrane also plays an important role in the separation process (van den Berg and Smolders, 1992).

In summary, Schofield *et al.* (1990) stated that any theoretical study of gas permeation through microporous structures begins with a comparison of the mean path of the gas and the mean pore size of the structure. If the mean free path of the gas is much less than the pores size, then the dominant flux mechanism is viscous or Poiseuille flow. If the mean free path is much greater than the pores size, then Knudsen diffusion is the dominant mechanism. A third mechanism encountered in gas permeation is surface diffusion, where gas molecules adsorb on the membrane walls and diffuse under a pressure gradient. This mechanism is not likely to be categorised under any of the previous mechanism and was considered to be a transition region between Knudsen and Poiseuille flow and was presented by equation (2-13).

As a conclusion, pore structure characterisation techniques are based on different principles. Different techniques measure different parameters of pore structure, which may not be comparable. It is, therefore, important to select the appropriate characterisation technique. There are several important factors that must be taken into consideration.

- I. *The pore structure characteristics required to be measured:* Pore structure has many characteristics including constricted through pore diameter, largest pore diameter, through pore volume, etc. The techniques suitable for measurement of those characteristics that are important for the application in hand need to be selected.
- II. *Limitations of the technique:* Each technique is appropriate to the measurement of a property within a certain range. Outside this range errors can be appreciable.
- III. *Constraint on test procedures:* Because of the nature of application there may be certain constraints on the testing process. For example toxic materials, high pressures and certain chemical environments are sometimes applied in these tests making the tested sample inoperative in further application processes. The selected technique must satisfy these constraints.
- IV. *Material stability:* The sample and the materials used in the test must not react with each other or with various components of the instrument.